UNIVERSIDADE DE SÃO PAULO

INSTITUTO DE FÍSICA
CAIXA POSTAL 20516
01498 - SÃO PAULO - SP
BRASIL

PUBLICAÇÕES

IFUSP/P-546

NUCLEAR SIZE EFFECTS IN VIRTUAL PHOTON SPECTRA

by

E. Wolynec, V.A. Serrão and M.N. Martins
Instituto de Física, Universidade de São Paulo

Setembro/1985

NUCLEAR SIZE EFFECTS IN VIRTUAL PHOTON SPECTRA

E. Wolynec, V.A. Serrão and M.N. Martins

Instituto de Física, Universidade de São Paulo
C.P. 20516, 01498 São Paulo, SP, Brazil

ABSTRACT

The (e,n) cross section has been measured for ^{181}Ta from threshold to 30 MeV. The results are compared with the cross sections predicted by virtual photon theory using different corrections for nuclear size effects.

[NUCLEAR REACTIONS: ^{181}Ta(e,n), E = 9-30 MeV; measured σ(E); virtual photon analysis; deduced E2 strength]

1. INTRODUCTION

During the last decade the study of the giant multipole resonances together with the emergence of distorted wave Born approximation (DWBA) virtual photon calculations of Onley, Wright, and collaborators[1,2] have jointly stimulated a renaissance of interest in electrodisintegration experiments. Early calculations of the M1, E2 and E3 virtual photon spectra in plane wave Born approximation (PWBA) showed that these spectra were greatly enhanced relative to the E1 spectrum. The enhancement was understood as resulting from the momentum dependence of higher multipole cross sections and the fact that in the electron scattering event the momentum transfer to the nucleus can greatly exceed the energy transfer. Experimental results[3-5] showed that these PWBA calculations were grossly underestimated for all but the lightest nuclei.

Gargaro and Onley[1] were the first to calculate the virtual photon spectra taking into account the distortion of the incoming and outgoing electron waves in the Coulomb field of a point nucleus. These calculations showed that the enhancement of higher multipole virtual photon spectra, already seen in PWBA calculations, was greatly increased as the atomic number of the nucleus increased.

The enhancement of the E2 relative to the E1 DWBA virtual photon spectra has recently been exploited in several electrodisintegration experiments to study E2 absorption by

nuclei (e.g. refs. 6-14). In these experiments the relationship between the electrodisintegration cross section $\sigma_{e,x}(E_0)$ and the photonuclear cross section $\sigma_{\gamma,x}(E)$ is used:

$$\sigma_{e,x}(E_0) = \int_0^{E_0-m} \sum_{\lambda L} \sigma_{\gamma,x}^{\lambda L}(E)\, N^{\lambda L}(E_0,E,Z)\, \frac{dE}{E} \qquad (1)$$

Here $N^{\lambda L}(E_0,E,Z)/E$ stands for the number of virtual photons of multipolarity λL exchanged with a nucleus of atomic number Z when an electron of energy E_0 produces an excitation of energy E.

Since the DWBA virtual photon spectra used in Eq. (1) are evaluated for a point nucleus, it is assumed that the transition probabilities for photodisintegration and electrodisintegration, $B(EL,E)$ and $B(EL,q)$, are equal. Here q is the momentum transferred to the nucleus in electrodisintegration. This assumption is exact as $q \to E$ but surely fails for $q \gg E$.

Several experimental checks of the DWBA virtual photon spectra have been made[3-5] but the most complete and accurate of these tests was an experiment performed at the National Bureau of Standards (NBS)[15]. An isochromat of the E1 virtual photon spectrum was measured by counting the number of ground-state protons emitted by the 16.28 MeV isobaric analog state in ^{90}Zr as a function of incident electron energy in the range 17-105 MeV. The experimental results reproduce

well the DWBA spectra for a point Zr nucleus for electron energies up to 30 MeV. A radiator was used for electron energies of 60-100 MeV to measure the photodisintegration cross section for the 16.28 MeV level. These results showed that the Davies-Bethe-Maximon bremsstrahlung cross section[16] yields the same result for $\Gamma_\gamma \Gamma_{p_0}/\Gamma$ as the electrodisintegration below 30 MeV, where size corrections for the finite extent of the Zr nucleus are minimal. As E_0 increases to 105 MeV the need for such corrections became manifest. It was shown that the size corrections of Dodge et al.[6] and of Durgapal and Onley[17] made the electrodisintegration results compatible with the photodisintegration results, for the full range of electron incident energies.

The size correction of Dodge et al.[6] consists in multiplying $N^{\lambda L}(E_0,E,Z)$ inside the integral of Eq. (1) by:

$$F^{\lambda L}(qR) = \left[\left(\frac{E}{q}\right)^L \frac{j_L(qR)}{j_L(ER)}\right]^2_{q=q_{rms}} \qquad (2)$$

where R is the radius of the nuclear ground state and q is the momentum transfer. The rms values of q are obtained in PWBA as described in ref. 6. This size correction is of the same magnitude as the one proposed by Shotter[18], also based on a PWBA calculation. For the electric dipole transition at 16.28 MeV in the ^{90}Zr nucleus $F^{\lambda L}(qR)$ is 0.89 for 100 MeV electrons and is negligible for electrons of less than 30 MeV.

Durgapal and Onley[17] take into account the size effects by evaluating the virtual photon spectra in second order Born approximation (SOBA) using a model for the nuclear charge and current density distributions. Their model reproduces values of the charge and transition radii obtained from electron scattering experiments. The resulting spectra are slightly smaller than those obtained with the use of Eq. (2).

The results obtained in the NBS experiment for $\Gamma_\gamma\Gamma_{p_0}/\Gamma$ are:

65.4 ± 0.6 eV from photodisintegration

66.1 ± 0.3 eV from electrodisintegration using SOBA

63.8 ± 0.3 eV from electrodisintegration using Eq. (2)

Eventhough both size corrections yield acceptable results, the result obtained with SOBA is closer to the photodisintegration result. The SOBA virtual photon calculation takes into account not only the fact that [B(EL,E)/B(EL,q)] is different from one, but also deviations from a point nuclear Coulomb field. Thus, in principle, results obtained with SOBA should be the most reliable.

However, SOBA cannot be used for heavy nuclei, because these require a full DWBA calculation. Onley and collaborators[19] have recently developed a DWBA calculation for the virtual photon spectra with size effects, using charge and current density distributions given by the Tassie hydrodynamical model[20]. The results of this calculation, which

are in agreement with the results from SOBA for Zr, show that for heavy nuclei size effects are important even at low electron incident energies (< 30 MeV).

Figs. 1 and 2 show E1 and E2 virtual photon spectra for E_0 = 12, 22 and 30 MeV and Z = 73. In these figures the solid lines represent the DWBA spectra for a point nucleus. The dashed lines represent the DWBA spectra with size effects[19]. For E1 the size effects decrease the spectra by ~ 10% and for E2 by ~ 50%.

The size correction based on PWBA calculations and given by Eq. (2) decreases the E1 spectra by 2% and the E2 spectra by 7% for E_0 = 30 MeV and virtual photons of 10 MeV. The correction becomes smaller for lower electron energies and also for higher virtual photon energies. These size corrections are much smaller than those shown in Figs. 1 and 2.

In order to test if the magnitude of the size corrections in the recent calculation of Onley and collaborators[19], which we will designate by DWBA-SZ, are in agreement with experimental results we have measured the electrodisintegration of ^{181}Ta.

2. THE EXPERIMENT

The ^{181}Ta(e,n) cross section was measured by residual activity, following the 93.3 KeV γ-ray line that

results from the decay of ^{180}Ta to ^{180}Hf, which has a half life of 8.11 ± 0.02 hours. We have used 7 targets obtained from two foils which were $\sim 4\ mg/cm^2$ and $\sim 10\ mg/cm^2$ thick. The target thicknesses, determined by weighing are listed in Table I. The targets were activated in the electron beam of the São Paulo Electron Linear Accelerator. The linac current was measured using a Faraday cup.

The measured cross section was corrected for the photodisintegration produced by bremsstrahlung in the targets. This correction was between 1 and 4% depending on the electron incident energy and the target thickness. For electron kinetic energies of 24, 27 and 30 MeV we have also measured the photodisintegration induced by bremsstrahlung, using a $0.329\ g/cm^2$ copper radiator, placed in the electron beam just ahead of the target. The linac current was measured using a secondary emission monitor calibrated relative to the Faraday cup. The measured yields were corrected for the energy loss of electrons in the radiator and the electrodisintegration produced in the targets was subtracted.

The results obtained for the electrodisintegration cross section are shown in Fig. 3. Each of the data points is the weighted mean of several measurements with different targets. The uncertainty in the absolute scale is 10 percent. The results obtained for the photodisintegration yield are given in Table II.

3. DISCUSSION

In order to compare our results with the predictions of virtual photon theory we have to discuss which multipoles should enter in evaluating Eq. (1). Besides the dominant E1, in the energy range covered by this experiment, there are several electric multipoles: the isoscalar E2 at $63\ A^{-1/3}$ MeV, the isoscalar E3 at $110\ A^{-1/3}$ MeV and the isovector E2 at $130\ A^{-1/3}$ MeV. Table III gives the integrated photonuclear cross sections corresponding to one energy weighted sum for each of these resonances. We have made the approximation:

$$\int \sigma_\gamma^{EL}(E)dE = E_p^{2L-2} \int \frac{\sigma_\gamma^{EL}(E)\,dE}{E^{2L-2}} \qquad (3)$$

where E_p is the peak position of the resonance.

Fig. 4 shows DWBA-SZ E1, E2 and E3 virtual photon spectra for 30 MeV electrons. Because the photonuclear cross section corresponding to one E3 sum is so much smaller than the E1 it makes neglegible contribution to our measured cross section, eventhough the E3 spectrum is enhanced relatively to the E1. Since electrons of the energies used here cannot excite the monopole giant resonance[21] we have to consider only E1 and E2 electric multipoles in Eq. (1).

The isoscalar E2 giant resonance in ^{181}Ta has been studied in (p,p') and (e,e') experiments. Table IV summarizes

the available results and suggests that these results are not in agreement as to the shape and strength. Fig. 5-a shows the photonuclear E2 cross section corresponding to the parameters given in Table IV. In Fig. 5-b the results of refs. (22) and (23) are normalized to the peak height of ref. (24) and it shows clearly that the three experiments are in good agreement as to the shape and position of the isoscalar E2 resonance. They disagree only in the strength, but this is a consequence of the different models used to extract it.

The isovector E2 was measured for ^{181}Ta by H. Miura et al.[24] and R.S. Hicks et al.[23]. Fig. 6 shows the predicted electrodisintegration yields for E1, isoscalar E2 and isovector E2. The E1 component was evaluated using the (γ,n) data from Livermore[25] in Eq. (1). For the isoscalar E2 we used a Lorentz line shape that reproduces the shape shown in Fig. 5-b and exhausts one sum. For the isovector E2 we used a Lorentz line shape with $E_p = 23.2$ MeV and $\Gamma = 7$ MeV, in accordance with ref. (23) with a strength corresponding to one sum to represent the E2 absorption, σ^{E2}_{abs}. However, since the isovector E2 is in a region where the dominant decay channel is $(\gamma,2n)$ we assumed that:

$$\sigma^{E2}_{\gamma,n} = \sigma^{E2}_{abs} \times \frac{\Gamma_n}{\Gamma_{tot}} = \sigma^{E2}_{abs} \times \frac{\sigma_{\gamma,n}}{\sigma_{\gamma,n} + \sigma_{\gamma,2n}} \qquad (4)$$

Since we are only interested in showing the relative magnitudes

of the various multipoles the yields shown in Fig. 6 were evaluated using DWBA virtual photon spectra for a point nucleus to speed up computing.

We have now to discuss the contributions from magnetic multipoles. Since there is no systematics for M1 and M2 absorption in heavy nuclei we assumed an M1 strength of $20\,\mu_0^2$ uniformly distributed between 7.6 and 8.6 MeV and for M2 we assumed the strength observed for ^{208}Pb[26]. The predicted yields are also shown in Fig. 6. It is clear that M2 can be neglected relatively to E1. The M1 can make a detectable contribution if a detailed measurement is performed in the threshold region. In the insert of Fig. 6 we illustrate the expected increase in the measured electrodisintegration cross section due to an M1 strength of $20\,\mu_0^2$ or to one E2 isoscalar sum, plotting the ratio of the predicted yields to a pure E1. The ratios shown were evaluated using DWBA-SZ.

From the above discussion we are led to take into account in the analysis of our experiment contributions from E1, E2 and M1.

The measured (γ,n) cross section[25] contains all multipoles but does not distinguish them. We can write:

$$\sigma_{\gamma,n}(E) = \sigma^{E1}_{\gamma,n}(E) + \sigma^{E2}_{\gamma,n}(E) + \sigma^{M1}_{\gamma,n}(E) \qquad (5)$$

and

$$\sigma^{E1}_{\gamma,n}(E) = \sigma_{\gamma,n}(E) - \sigma^{E2}_{\gamma,n}(E) - \sigma^{M1}_{\gamma,n}(E) \qquad (6)$$

Inserting (6) in (1) we write:

$$\sigma_{e,n}(E_0) = k_1 \int_0^{E_0-m} \sigma_{\gamma,n}(E)\, N^{E1}(E_0,E,Z)\, \frac{dE}{E} +$$

$$+ k_2 \int_0^{E_0-m} \sigma^{E2}_{\gamma,n}(E) \left[N^{E2}(E_0,E,Z) - N^{E1}(E_0,E,Z) \right] \frac{dE}{E} +$$

$$+ k_3 \int_0^{E_0-m} \sigma^{M1}_{\gamma,n}(E) \left[N^{M1}(E_0,E,Z) - N^{E1}(E_0,E,Z) \right] \frac{dE}{E} \qquad (7)$$

where for $\sigma_{\gamma,n}(E)$ we use the measured (γ,n) cross section[25] and k_i are constants to be determined from the fit of Eq. (7) to our data.

The constant k_1 allows for a difference between our absolute scale and that of the (γ,n) cross section. This constant can also be determined, independently, by comparing our measured bremsstrahlung yield given in Table III with the calculated values:

$$\sigma_{Br,n} = N_r \int_0^{E_0-m} \sigma_{\gamma,n}(E)\, K(E_0,E,Z)\, \frac{dE}{E} \qquad (8)$$

where $\sigma_{\gamma,n}$ is the photonuclear cross section[25], K is the Davies-Bethe-Maximon bremsstrahlung cross section[16] and N_r

is the number of nuclei/cm^2 in our radiator. Using Eq. (8), k_1 is the ratio between measured and calculated yields. From our measurements we obtain $k_1 = 1.29 \pm 0.04$.

For $\sigma^{E2}_{\gamma,n}$ isoscalar and isovector we have used the shapes previously discussed and used to evaluate the yields of Fig. 6. Thus, by fitting Eq. (7) to our data, k_2 will give the fraction of the E2 isovector and isoscalar sums.

For $\sigma^{M1}_{\gamma,n}$ we assumed a strength of $1\,\mu_0^2$ uniformily distributed between 7.6 and 8.6 MeV excitation energy, since the M1, if it is located above the (γ,n) threshold, will be distributed into many levels and our measurement is not sensitive to the detailed structure. In Eq. (7) k_3 will give the M1 strength in units of μ_0^2.

We fitted our electrodisintegration data with Eq. (7) using the DWBA virtual photon spectra corrected for size effects with Eq. (2) and obtained a good fit with $k_1 = 1.16 \pm 0.02$, an E2 intensity of (70 ± 10) percent of the E2 sum and an M1 intensity of $(17 \pm 5)\,\mu_0^2$. The quality of the fit was good and the results would seem quite reasonable. However, this result is unacceptable, since the value of k_1 obtained from the fit is incompatible with the value determined from our photodisintegration measurements. This is an important point and could explain why previous results of electrofission measurements, analized with DWBA virtual photon spectra for a point nucleus yielded conflicting results. (See for example refs. 12-14). A measurement of the photodisintegration yield,

under the same experimental conditions as the electrodisintegration, is a necessary constraint.

It is impossible to fit our electrodisintegration data using $k_1 = 1.29 \pm 0.04$ and the DWBA virtual photon spectra for a point nucleus or corrected for size effects by Eq. (2). Fig. 7-a shows the ratio of measured to calculated electrodisintegration for E1 only ($k_1 = 1.29$, $k_2 = k_3 = 0$) (using the size corrections of Eq. (2)). Since the ratio becomes smaller than one, it would require negative E2 and/or M1 strength to fit the data. The conclusion is that with this size correction photo and electrodisintegration are incompatible. Fig. 7-b shows the same ratio evaluated with DWBA-SZ. The ratio is greater than one indicating that other multipoles contribute.

We fitted our data using DWBA-SZ for the virtual photon spectra in Eq. (7). Since it turned out that k_3 was compatible with zero, we fitted the data only in terms of E1 and E2. The solid curve in Fig. 3 is the result of this fit. The results obtained are: $k_1 = 1.31 \pm 0.02$ and an E2 strength of 140 ± 37 percent of the isoscalar E2 sum and 31 ± 8 percent of the isovector E2 sum in the (γ,n) channel. Fig. 7-c shows the ratio of measured to calculated yield. The agreement is excellent.

The DWBA calculation for a finite nucleus from Onley and collaborators[19] makes electro and photodisintegration yields compatible since it yields the same value for k_1 as obtained, independently, from our photodisintegration measurements.

The isoscalar E2 intensity is consistent with the sistematics for heavy nuclei[27,28]. The uncertainty in the E2 strength could be decreased by extending the measurement to higher electron incident energies.

The fact that the present measurement is consistent with the absence of M1 does not exclude the possibility of M1 strength near threshold. Actually in the ratio shown in Fig. 7-c the first point is high as expected when there is M1. In order to be more conclusive about the M1 component we would need to measure several points from threshold to 9 MeV with good statistics.

CONCLUSIONS

Our results indicate that the recent calculation of DWBA virtual photon spectra for a finite nucleus is in agreement with experimental results. With these calculations photo and electrodisintegration results are compatible. For heavy nuclei the difference between the spectra for a finite and point nucleus is large for the E2 spectra even for electron energies around 10 MeV. This invalidates the multipole decomposition obtained in several previous experiments of electrodisintegration and electrofission in heavy nuclei.

Since the analysis of electrodisintegration experiments in terms of virtual photon spectra involves, usually, a

photonuclear cross section measured in an independent experiment, reliable results can only be obtained if the possibility of differences between the absolute scales of the electrodisintegration and photodisintegration cross sections are taken into account.

The authors wish to acknowledge to D.S. Onley for computing the DWBA virtual photon spectra for a finite nucleus necessary to the analysis of the present work and the financial support from Fundação de Amparo à Pesquisa do Estado de São Paulo, Conselho Nacional de Desenvolvimento Científico e Tecnológico e Financiadora de Estudos e Projetos.

REFERENCES

1. W.W. Gargaro and D.S. Onley, Phys. Rev. C4 (1971) 1032.
2. C.W. Soto Vargas, D.S. Onley, and L.E. Wright, Nuc. Phys. A288 (1977) 45.
3. I.C. Nascimento, E. Wolynec, and D.S. Onley, Nucl. Phys. A246 (1975) 210.
4. E. Wolynec, G. Moscati, M.N. Martins, and O.D. Gonçalves, Nucl. Phys. A244 (1975) 205.
5. E. Wolynec, G. Moscati, J.R. Moreira, O.D. Gonçalves, and M.N. Martins, Phys. Rev. C11 (1975) 1083.
6. E. Wolynec, W.R. Dodge, R.G. Leicht, and E. Hayward, Phys. Rev. C22 (1980) 1012.
7. W.R. Dodge, R.G. Leicht, E. Hayward, and E. Wolynec, Phys. Rev. C24 (1981) 1952.
8. D.M. Skopik, J. Asai, and J.J. Murphy II, Phys. Rev. C21 (1980) 1746.
9. T. Tamae, T. Urano, M. Hirooka, and M. Sugawara, Phys. Rev. C21, 1758 (1980).
10. A.G. Flowers, D. Branford, J.C. McGeorge, A.C. Shotter, P. Thorley, and C.H. Zimmerman, Phys. Rev. Lett. 43 (1979) 323.
11. J.D.T. Arruda-Neto, S.B. Herdade, I.C. Nascimento, and B.L. Berman, Nucl. Phys. A389 (1982) 378.
12. J. Aschenbach, R. Haeg, and H. Krieger, Z. Phys. A292 (1979) 285.

13. H. Stroher, R.D. Fisher, J. Drexler, K. Huber, U. Kneissl, R. Batzek, H. Ries, W. Wilcke, and H.J. Maier, Phys. Rev. Lett. 47 (1981) 318.

14. H. Stroher, R.D. Fisher, J. Drexler, K. Huber, U. Kneissl, R. Batzek, H. Ries, W. Wilke, and H.J. Maier, Nucl. Phys. A378 (1982) 237.

15. W.R. Dodge, E. Hayward, and E. Wolynec, Phys. Rev. C28 (1983) 150.

16. J.L. Mathews and R.O. Owens, Nucl. Instr. Methods 111 (1973) 157.

17. P. Durgapal and D.S. Onley, Bull. Am. Phys. Soc. 27 (1982) 487; P. Durgapal, Ph.D. dissertation, Ohio University, Ohio, 1982; private communication.

18. A.C. Shotter, J. Phys. G5 (1979) 371.

19. Farid Zamani-Noor, Ph.D. dissertation, Ohio University, Ohio, 1984 and D.S. Onley, private communication.

20. L.J. Tassie, Austral. J. Phys. 9 (1956) 407.

21. E. Hayward, in Giant Monopole Resonances, edited by Fred E. Bertrand (Harwood Academic, New York, 1980).

22. N. Marty, M. Morlet, A. Willis, V. Comparat, and R. Frascaria, Nucl. Phys. A238 (1975) 93.

23. R.S. Hicks, I.P. Auer, J.C. Bergstron, and H.S. Caplan, Nucl. Phys. A278 (1977) 261.

24. H. Miura and Y. Torizuka, Phys. Rev. C16 (1977) 1688.

25. R.L. Bramblett, J.T. Caldwell, G.F. Auchampaugh, and S.C. Fultz, Phys. Rev. 129 (1963) 2723.

26. R.S. Hicks, R.L. Huffmann, R.A. Lindgren, B. Parker, and G.A. Peterson, Phys. Rev. C26 (1982) 920.

27. F.E. Bertrand, Nucl. Phys. A354 (1981) 129c.

28. F.E. Bertrand, Ann. Rev. Nucl. Sci. 26 (1976) 457.

FIGURE CAPTIONS

Fig. 1 – DWBA E1 virtual photon spectra for E_0 = 12, 22 and 30 MeV for a point and a finite nucleus.

Fig. 2 – DWBA E2 virtual photon spectra for E_0 = 12, 22 and 30 MeV for a point and a finite nucleus.

Fig. 3 – Measured electrodisintegration cross section versus the electron kinetic energy. The uncertainty in the absolute scale is 10 percent. Each data point is the weighted mean of several measurements. The solid curve is a fit of the data, with E1 and E2 components in the (γ,n) cross section, using DWBA virtual photon spectra for a finite nucleus.

Fig. 4 – E1, E2 and E3 DWBA virtual photon spectra for a finite nucleus.

Fig. 5 – a) Experimental results for the isoscalar E2 resonance in ^{181}Ta. b) The results shown in a) are normalized to the same peak height.

Fig. 6 – The contributions of various multipoles to the electrodisintegration cross section (see text for details). The insert shows the ratio of calculated yields for (E1+M1) and (E1+E2) to pure E1.

Fig. 7 – Ratio of measured to calculated electrodisintegration cross section. a) Using DWBA virtual photon spectra corrected for size effects with Eq. (2) and assuming that the (γ,n) cross section is pure E1. b) Using DWBA virtual photon spectra for a finite nucleus and assuming that the (γ,n) cross section is pure E1. c) Using DWBA virtual photon spectra for a finite nucleus and assuming that the (γ,n) cross section contains contributions from both E1 and E2.

TABLE I

Target thickness

Target	Thickness (mg/cm^2)
1	3.82 ± 0.12
2	3.81 ± 0.11
3	3.84 ± 0.12
4	10.19 ± 0.30
5	10.23 ± 0.31
6	10.24 ± 0.31
7	10.34 ± 0.31

TABLE II

Photodisintegration yield obtained with a 0.329 g/cm^2 radiator

Number of measurements	Electron kinetic energy (MeV)	$\sigma_{Br,n}$ (mb)
6	24	2.74 ± 0.06
4	27	2.61 ± 0.06
6	30	3.01 ± 0.06

TABLE III

Integrated photonuclear cross sections

λL	T	E_p (MeV)	$\int \sigma_\gamma^{EL}(E)\,dE$ (MeV . mb)
E1	1	$80\ A^{-1/3}$	2613
E2	0	$63\ A^{-1/3}$	27
E2	1	$130\ A^{-1/3}$	162
E3	0	$110\ A^{-1/3}$	1

TABLE IV

Isoscalar E2 resonance

Reaction	E_p (MeV)	Γ (MeV)	% EWSR	Ref.
(p,p')	11.2 ± 0.2	3.9	42 ± 8	22
(e,e')	9.54 ± 0.20	2.07 ± 0.35	8 ± 4	23
	11.47 ± 0.22	3.13 ± 0.55	22 ± 8	
(e,e')	9.5 ± 0.2	1.8 ± 0.6	29 ± 5	24
	11.3 ± 0.2	2.2 ± 0.7	63 ± 8	
	12.6 ± 0.2	1.3 ± 0.8	11 ± 5	

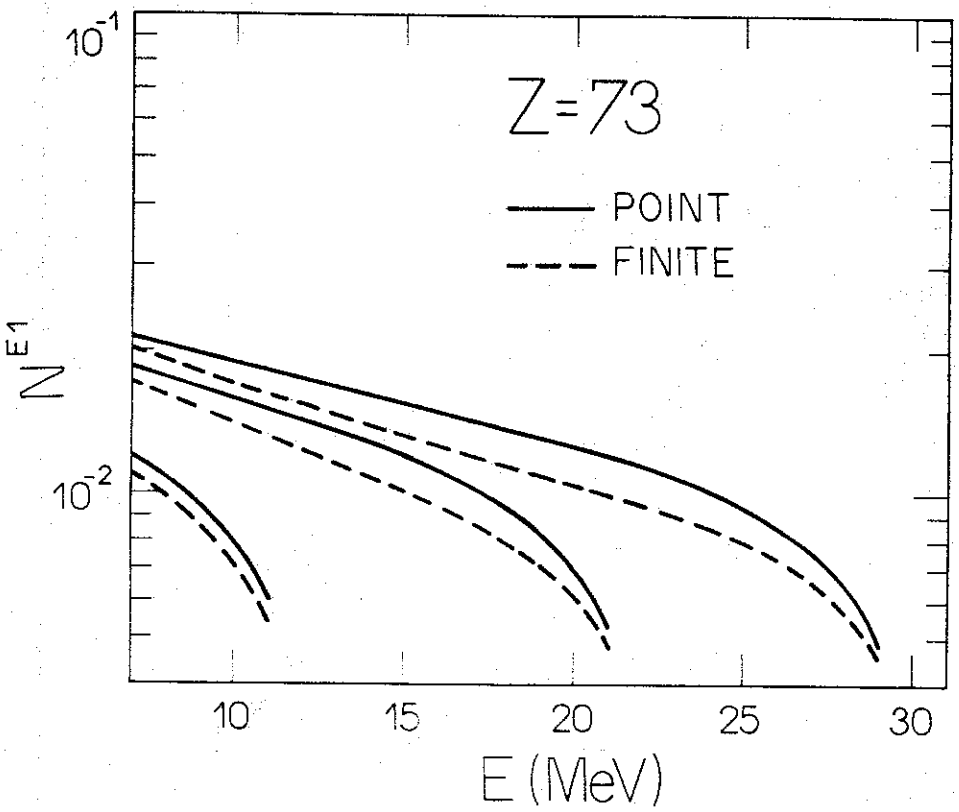
Z=73
POINT
FINITE
10^{-1}
10^{-2}
N^{E1}
10
15
20
25
30
E (MeV)

FIG. 1

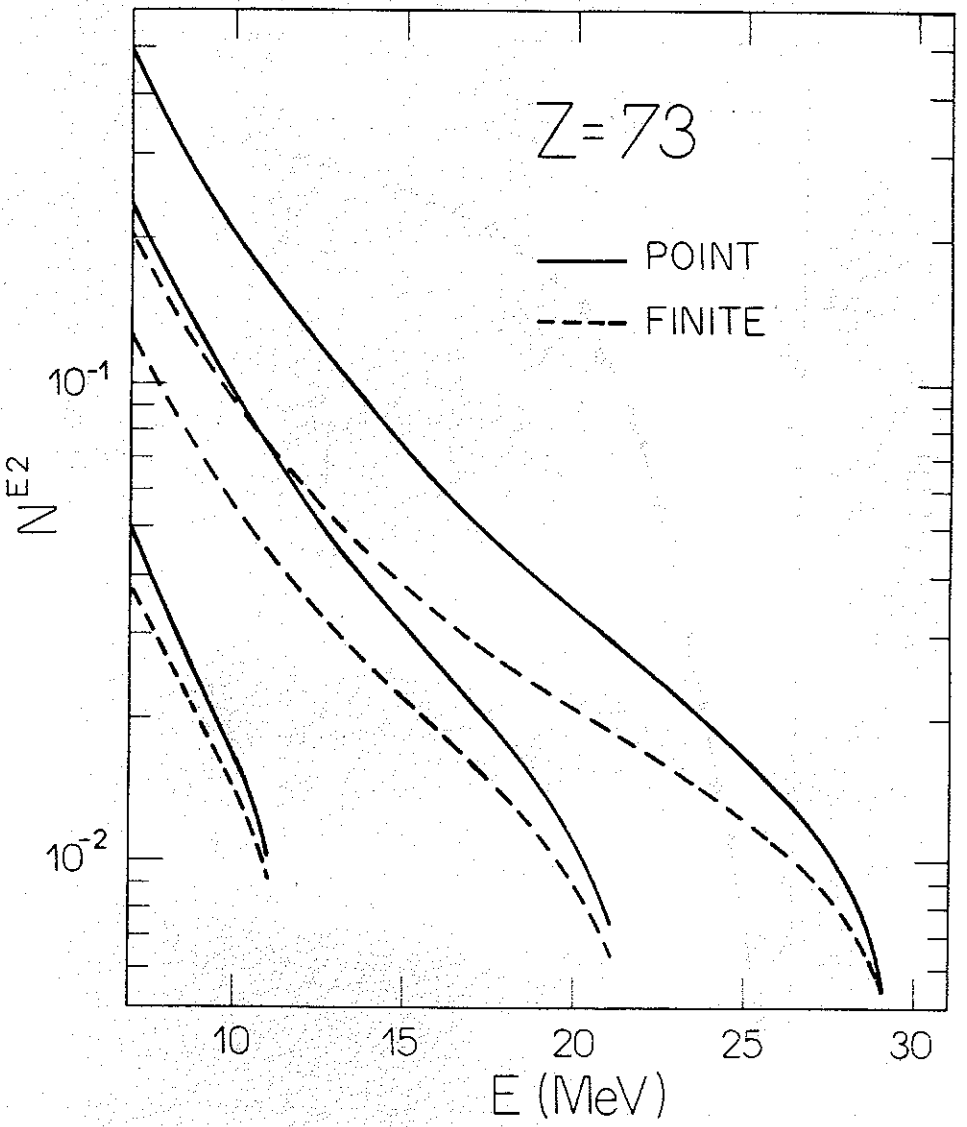
Z=73
POINT
FINITE
10^{-1}
10^{-2}
N^{E2}
10
15
20
25
30
E (MeV)

FIG. 2

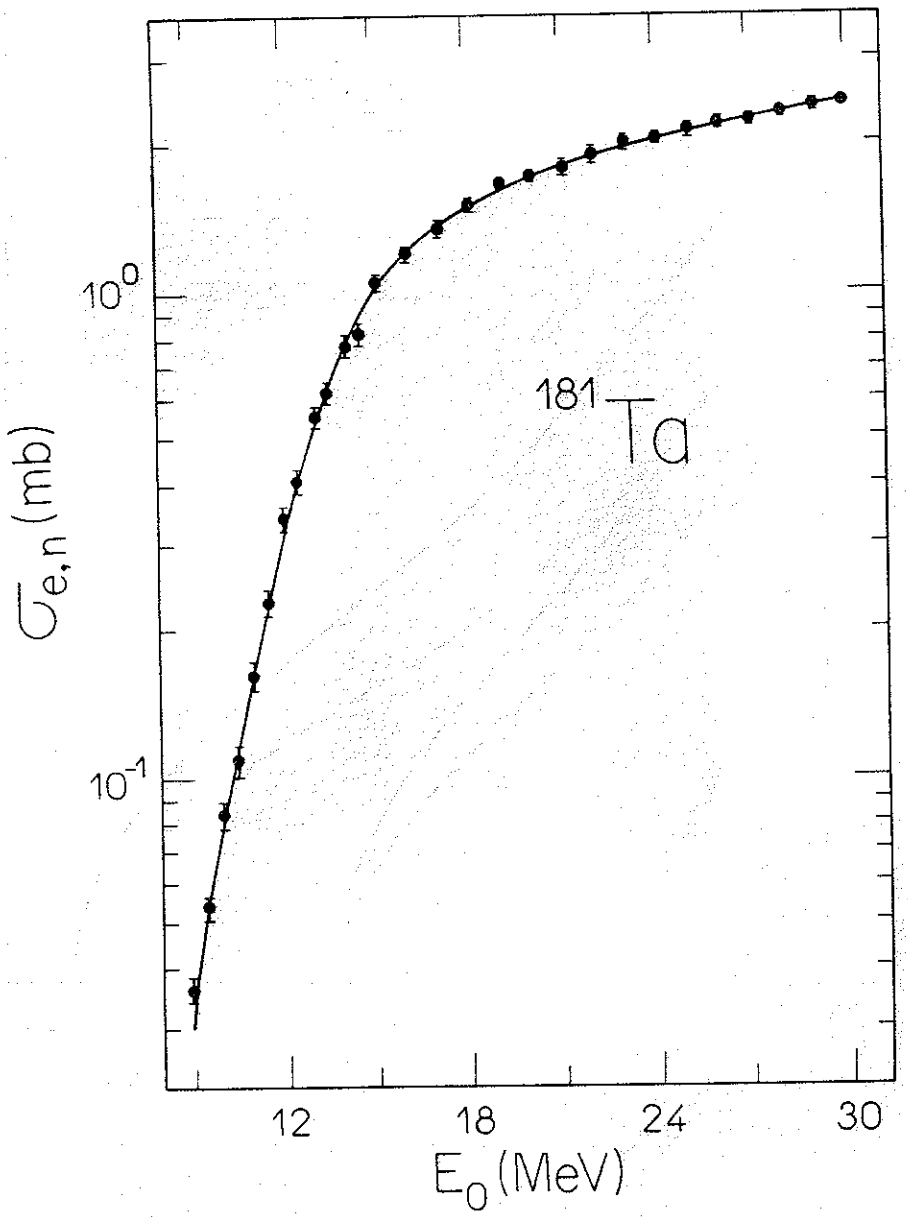
$\sigma_{e,n}$ (mb)
10^0
10^{-1}
^{181}Ta
12
18
24
30
E_0 (MeV)

FIG. 3

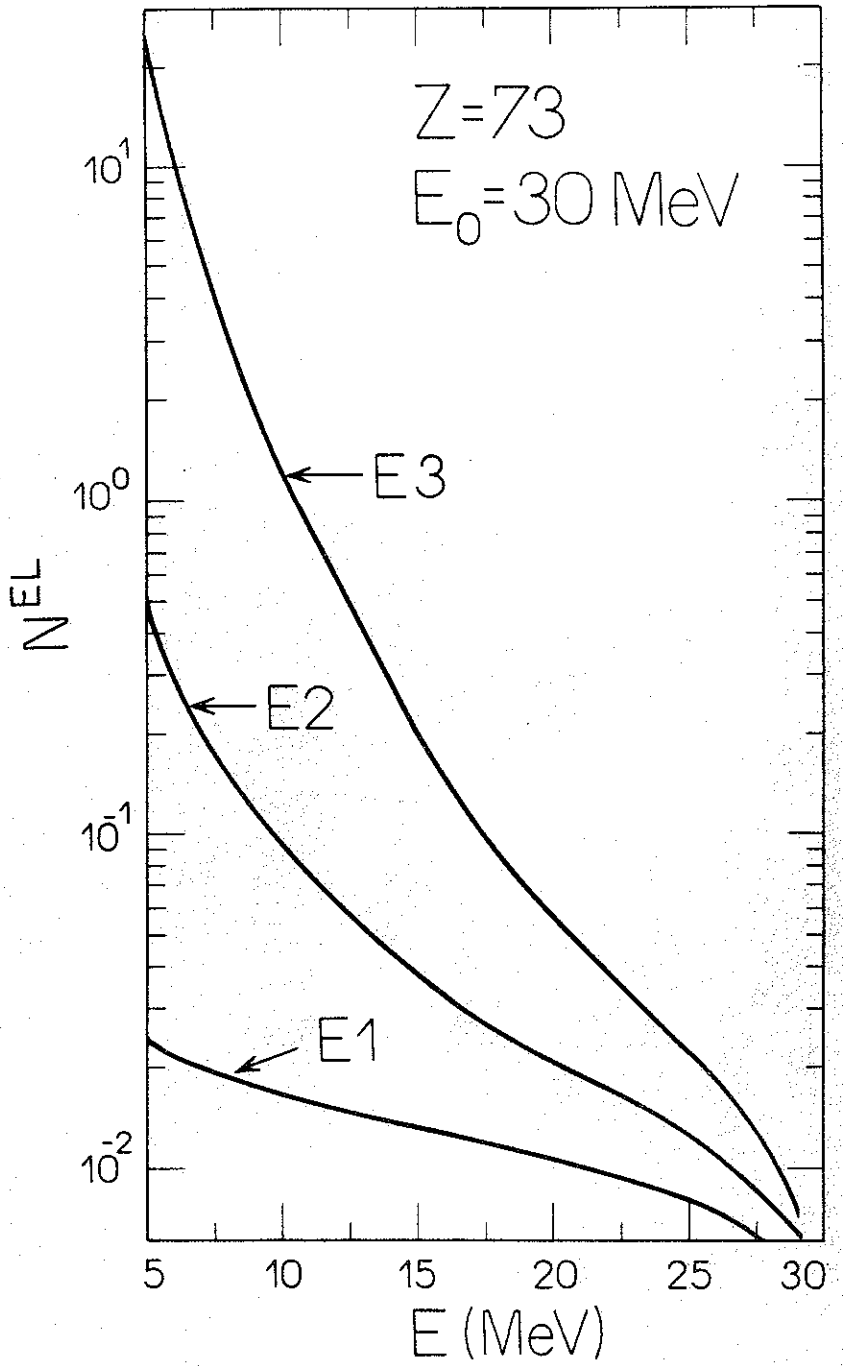
Z=73
E_0=30 MeV
N^{EL}
10^1
10^0
10^{-1}
10^{-2}
E3
E2
E1
5
10
15
20
25
30
E (MeV)

FIG. 4

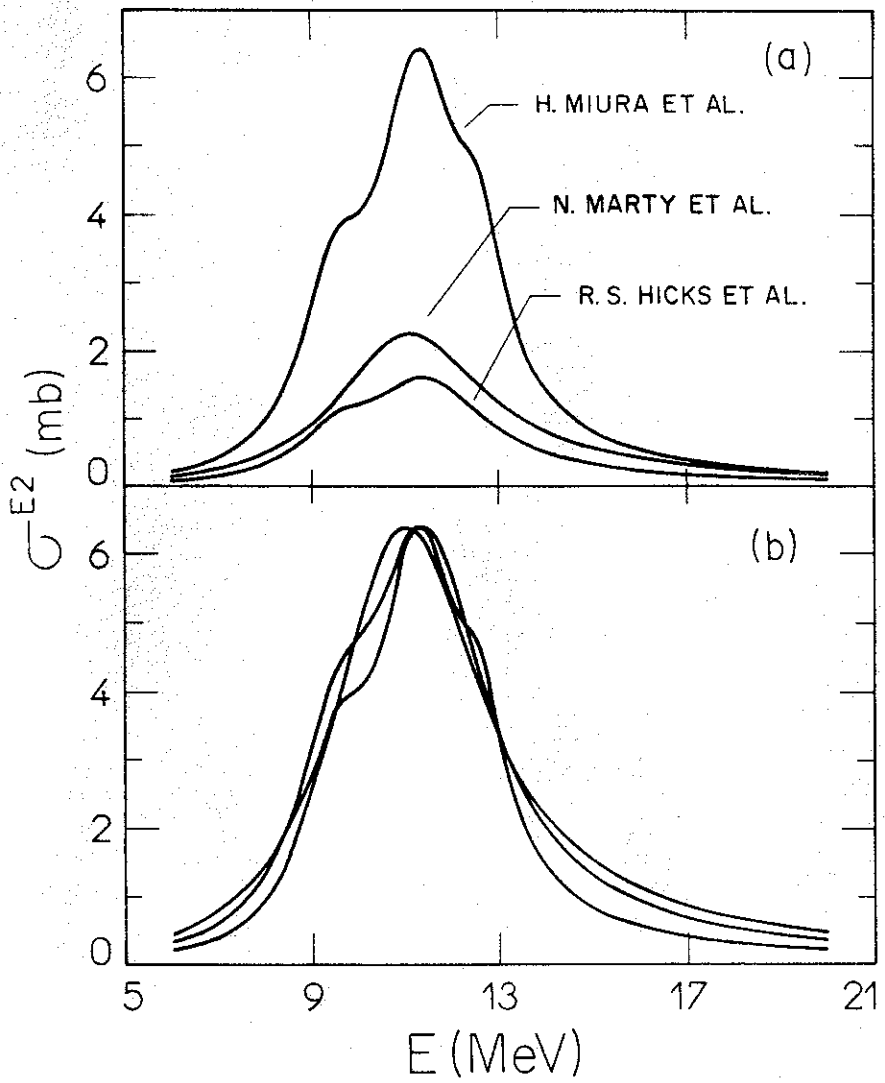
(a)
H. MIURA ET AL.
N. MARTY ET AL.
R. S. HICKS ET AL.
(b)
σ^{E2} (mb)
E (MeV)

FIG. 5

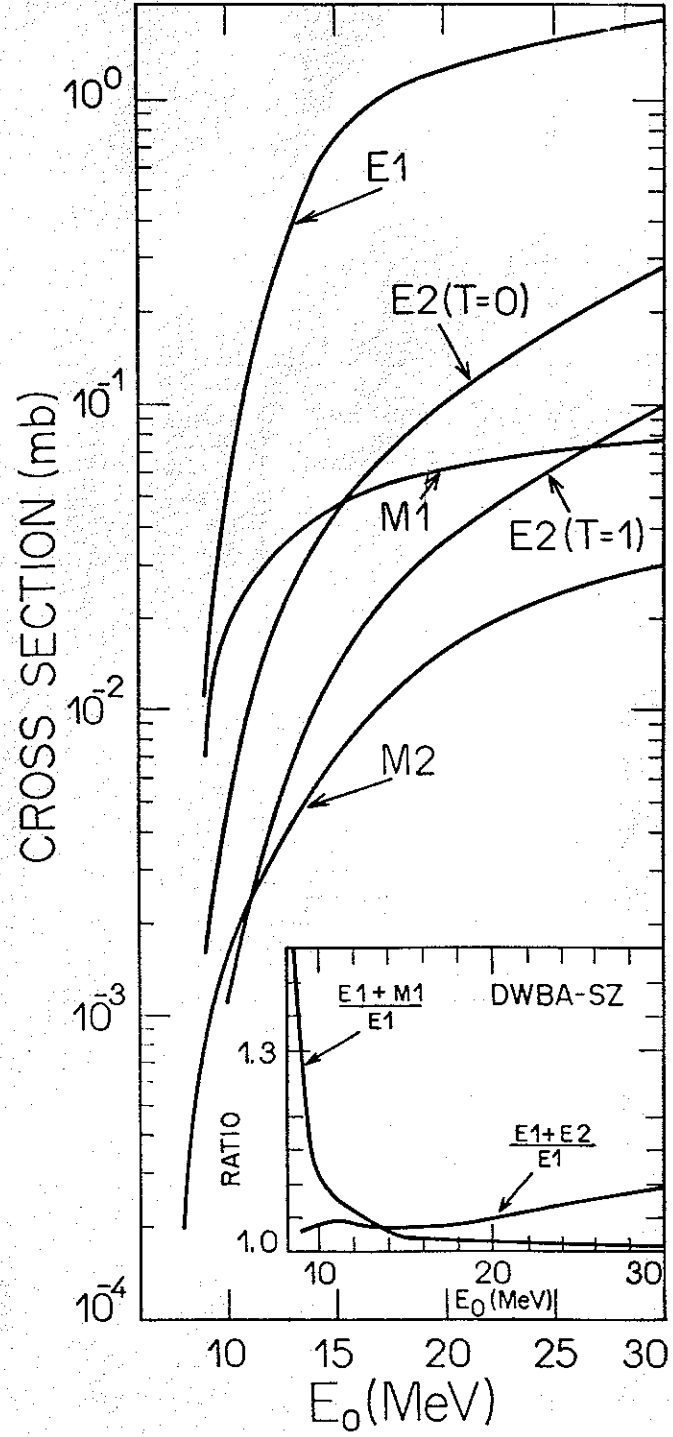
E1
E2(T=0)
M1
E2(T=1)
M2
CROSS SECTION (mb)
E1 + M1 / E1
DWBA-SZ
E1+E2 / E1
RATIO
E_0 (MeV)
E_0 (MeV)

FIG. 6

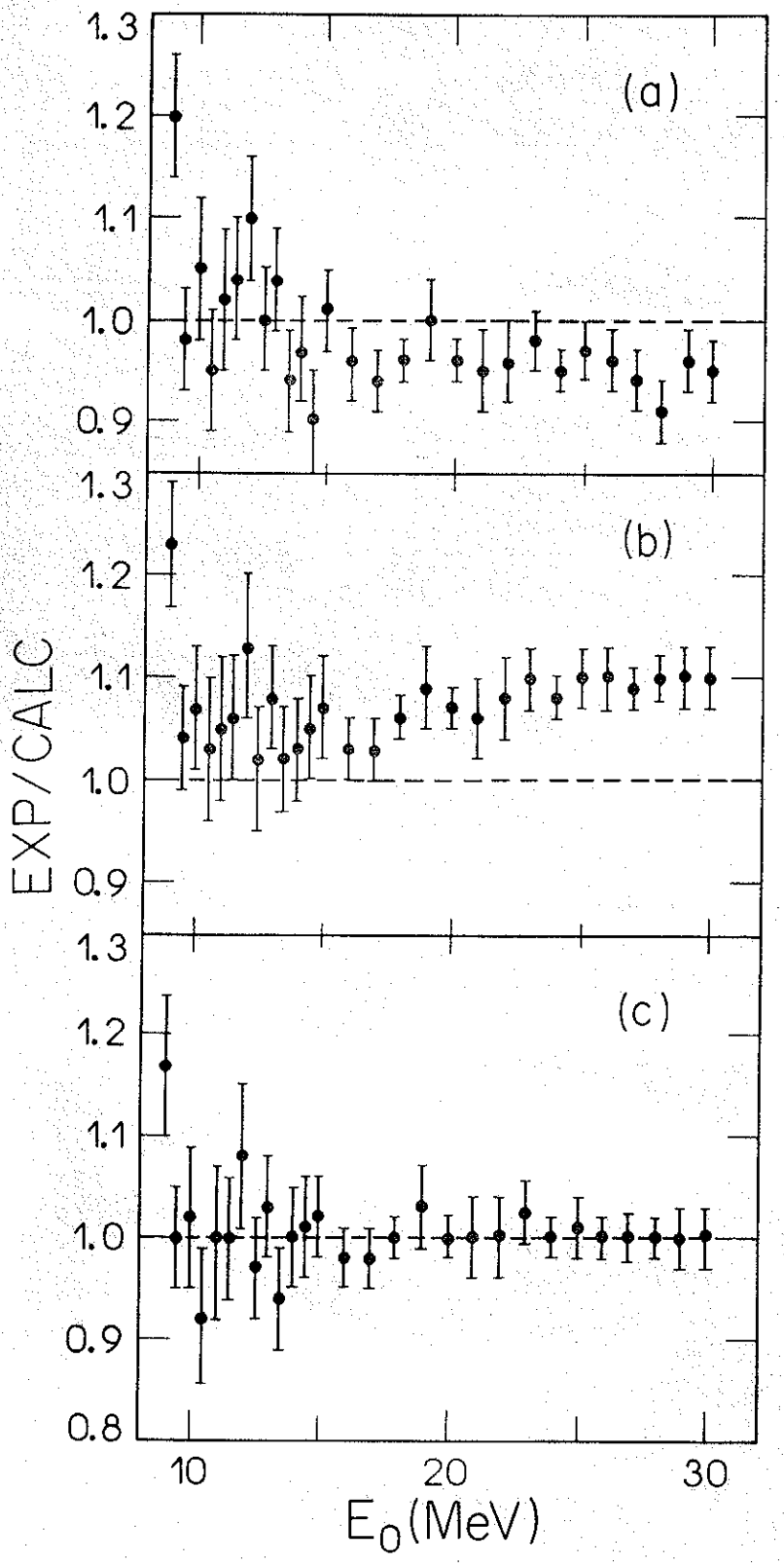

FIG. 7